2016 16th International Conference on Control, Automation and Systems (ICCAS 2016)
Oct. 16-19, 2016 in HICO, Gyeongju, Korea

Optimal Brake Distribution for Electronic Stability Control Using Weighted Least Square Allocation Method

Giseo Park and Seibum B. Choi*

School of Mechanical Aerospace & Systems Engineering, Division of Mechanical Engineering,
Korea Advanced Institute of Science and Technology, Daejeon, Korea
(Tel: +82-42-350-4160; E-mail: giseo123@kaist.ac.kr, sbchoi@kaist.ac.kr)

Abstract: Electronic stability control (ESC) system is well known as a method to assist the driver in recovering from unintended situations, such as understeering and oversteering behaviors. One of issues of this ESC is precise distribution of the brake force for generation of the vehicle yaw moment. In this paper, a new design of ESC systems is proposed. First, the model based controller with vehicle bicycle model computes the correction yaw moment, which makes the vehicle follow the desired yaw rate. Then, weighted least squares (WLS) allocation method minimizing the user-defined cost function with equality constraints is implemented for generation of the brake pressures of individual wheels. In addition, taking both weight shifting caused by pitching motion of the vehicle body and minimum disturbance of longitudinal dynamics into account, the limits of brake pressures are managed in real time. The performances of the proposed algorithm are verified in the simulation environments using Carsim and Matlab/Simulink.

Keywords: electronic stability control, model based control, weighted least squares allocation, brake distribution

1. INTRODUCTION

Over the past two decades, vehicle control systems for improved vehicle handling and safety have been introduced from the research community and car manufacturers [1]. Among them, the electronic stability control (ESC) system is known as one of effective ways to maintain the vehicle yaw stability [1]-[2]. When the losses of steering control, such as understeering and oversteering are detected, ESC systems intervene to assist the driver in recovering from dangerous situations. The national highway and traffic safety administration (NHTSA) in the U.S. issued that ESC reduces crash accidents by 35% [3]. Generally, ESC systems are designed to be activated whenever the differences between desired and actual yaw rates become over a threshold [1], [4]. Taking vehicle states, road conditions and driver maneuvers into account, the required correction yaw moment generated by brake pressures of each individual wheel is determined by the ESC controller. When the clockwise yaw moment is required, the brake actuators at only right side wheels are automatically actuated. On the other wise, those at only left side wheels are actuated when counter-clockwise yaw moment is required. Some previous papers proposed the ESC algorithms based on the vehicle bicycle model or the full car model [1]-[2], [5]-[6]. Fortunately, through some estimation algorithms [7], it is possible to design the ESC controller with the readily available sensors of commercial vehicles, such as 6D-IMU, wheel speed sensor, steering angle sensor, and brake pressure sensor.

During the normal braking, the ratio of brake pressures between the front and rear wheels is constant due to unchanged proportional valve gain. On the contrary, while ESC systems are implemented, the brake pressures at front and rear wheels of same side are automatically distributed with an optimal ratio, which consider the physical limits of the brake actuators. The brake distribution with the optimal ratio can yield both vehicle stability and minimum disturbance of vehicle longitudinal motion. However, this brake distribution between front and rear wheels is not fully studied in the previous papers in regard to ESC systems.

In this paper, to minimize the difference between desired and actual correction yaw moment, a method for optimal distribution of brake pressures in real time is proposed. In addition, this method can minimize the effort of brake actuators: it is useful for improvement of energy efficiency. For this purpose, control allocation algorithm dealing with control of overactuated systems is exploited [8]. Among them, weighted least squares (WLS) is applied for brake control allocation. Overall architecture is illustrated in Fig. 1.

To evaluate the effectiveness of the proposed algorithm, the tracking error of yaw rate with and without ESC systems are analyzed together. Also, the generated yaw moment and the ratio of the brake pressures are simultaneously observed and analyzed.

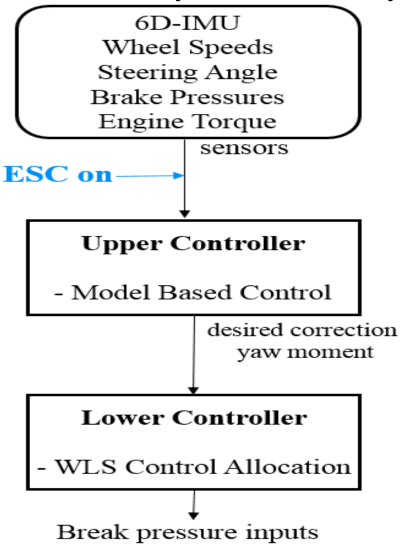

Fig. 1 Overall architecture.

Vehicle dynamics software, Carsim and Matlab/Simulink are used for evaluation and verification in this paper.

2. VEHICLE DYNAMICS

2.1 Vehicle dynamic model

As shown in Fig. 2, the bicycle model indicates vehicle lateral dynamics in an assumption that wheels are located at the vehicle center line [1]. The dynamic equations of the bicycle model in terms of force balance and moment balance are expressed as follows:

$$\mathrm{m v_x}(\dot{\beta} + \mathrm{r}) = \mathrm{F_{yf}} + \mathrm{F_{yr}} \tag{1}$$

$$\mathrm{I_z}\,\dot{\mathrm{r}} = \mathrm{F_{yf}}\,\mathrm{l_f} - \mathrm{F_{yr}}\,\mathrm{l_r} + M_z \tag{2}$$

where β is the body side slip angle, r the yaw rate, m the vehicle mass, I_z the vehicle yaw moment of inertia, v_x the vehicle longitudinal speed, and M_z the correction yaw moment. l_f and l_r are the CG-front and CG-rear axle distances, F_{yf} and F_{yr} the lateral tire forces of front and rear axle, respectively. The lateral tire forces can be expressed as linearly proportional to α_*, side slip angle of tire.

$$F_{yf} = -C_f \alpha_f \tag{3}$$

$$F_{yr} = -C_r \alpha_r \tag{4}$$

where C_f and C_r denote the lumped cornering stiffness of front and rear tires, respectively. For constant or slowly varying longitudinal speed, the side slip angles of tires are expressed as

$$\alpha_f = \beta + \frac{l_f}{v_x} r - \delta_f \tag{5}$$

$$\alpha_r = \beta - \frac{l_r}{v_x} r \tag{6}$$

where δ_f is average of the front steering angles.

By augmenting (1)-(6), state-space expression of the bicycle model is given as follows :

$$\begin{bmatrix} \dot{\beta} \\ \dot{r} \end{bmatrix} = \begin{bmatrix} -\dfrac{C_f + C_r}{m v_x} & \dfrac{C_r l_r - C_f l_f}{m v_x^2} - 1 \\ \dfrac{C_r l_r - C_f l_f}{I_z} & -\dfrac{C_f l_f^2 + C_r l_r^2}{I_z v_x} \end{bmatrix} \begin{bmatrix} \beta \\ r \end{bmatrix} + \begin{bmatrix} \dfrac{C_f}{m v_x} \\ \dfrac{C_f l_f}{I_z} \end{bmatrix} \delta_f + \begin{bmatrix} 0 \\ \dfrac{M_z}{I_z} \end{bmatrix} \tag{7}$$

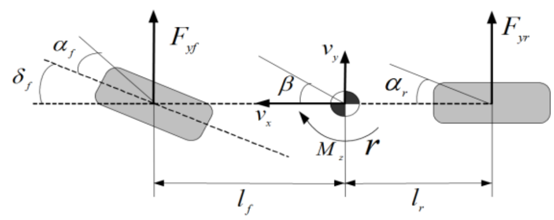

Fig. 2 Diagram of vehicle bicycle model.

2.2 Controller design

The upper controller is designed to achieve the nominal yaw rate motion and prevent oversteering and understeering [5]. Vehicle motion behaviour is shown in Fig. 3, and three possibilities of steady state cornering are classified as follows:

$$\begin{array}{ll} |\alpha_f| > |\alpha_r| & \text{understeering} \\ |\alpha_f| = |\alpha_r| & \text{neutral steering} \\ |\alpha_f| < |\alpha_r| & \text{oversteering} \end{array} \tag{8}$$

The desired yaw rate can be expressed as function of steering angle δ_f and vehicle longitudinal speed v_x [9]. It is represented as follows:

$$r_{des} = \frac{v_x}{l_f + l_r + \dfrac{m v_x^2 (l_r C_r - l_f C_f)}{2 C_f C_r (l_f + l_r)}} \delta_f \tag{9}$$

To follow the desired yaw rate, the sliding surface is determined as the tracking error of the yaw rate.

$$s = r - r_d \tag{10}$$

Consider a Lyapunov function candidate V, positive definite [10].

$$V = \frac{1}{2} s^2 \tag{11}$$

For negative definite $\dot{V}$, let $\dot{s}$ be as follows:

$$\dot{s} = -\eta s \tag{12}$$

where η is positive constant.

By substituting $\dot{r}$ in (7), the time derivation of s can be obtained as

$$\begin{aligned} \dot{s} &= -\eta s \\ &= \frac{C_r l_r - C_f l_f}{I_z} \beta - \frac{C_f l_f^2 + C_r l_r^2}{I_z v_x} r + \frac{C_f l_f}{I_z} \delta_f + \frac{M_z}{I_z} - \dot{r}_d \end{aligned} \tag{13}$$

Therefore, the control input M_z is given as follows:

$$\begin{aligned} M_z &= I_z \dot{r}_d + (C_f l_f - C_r l_r) \beta \\ &\quad + \frac{C_f l_f^2 + C_r l_r^2}{v_x} r - C_f l_f \delta_f - \eta I_z (r - r_d) \end{aligned} \tag{14}$$

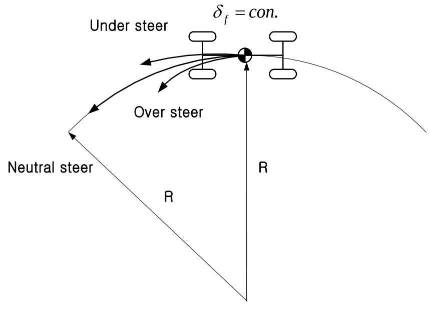

Fig. 3 Steady state cornering.

3. ELECTRONIC STABILITY CONTROL

3.1 Generation of correction yaw moment

In the lower controller, control input in (14) consists of the individual tire forces generated by the differential braking system [9]. As shown in Fig. 4, the correction yaw moment is obtained as follows:

$$M_z = t\cdot\cos(\delta_f)\cdot(F_{x,R1}-F_{x,L1})+l_f\cdot\sin(\delta_f)\cdot(F_{x,R1}+F_{x,L1}) \\ +t\cdot\sin(\delta_f)\cdot(F_{y,L1}-F_{y,R1})+t\cdot(F_{x,R2}-F_{x,R1}) \quad (15)$$

Assuming that the steering angle is small, $\sin(\delta_f)$ is assumed to be zero. Equation (15) is rewritten as follows:

$$M_z = t\cdot\cos(\delta_f)\cdot(F_{x,R1}-F_{x,L1})+t\cdot(F_{x,R2}-F_{x,L2}) \quad (16)$$

To identify the longitudinal tire force of each wheel, wheel rotational dynamics is utilized.

$$F_{x,i} = \frac{J_\omega\dot{\omega}_i + T_{b,i} - T_{d,i}}{R_e} + \mu_r F_{z,i} \quad (i = L1, L2, R1, R2) \quad (17)$$

T_d and T_b are the drive torque and the brake torque, respectively. R_e is the effective wheel radius, J_w the moment of inertia of a wheel, F_z the vertical tire force, and μ_r the rolling resistance coefficient. As mentioned above, according to the steering characteristics, the brake forces at left or right sides are generated during left turn (see Fig. 5). In the normal braking situation, the ratio of front-to-back distribution of brake pressures of same side is fixed due to constant pressure proportioning valve in the hydraulic systems. On the contrary, this ratio is ignored while ESC systems are implemented. By substituting for $F_{x,L1}$ and $F_{x,L2}$ in (16), the brake distribution for counter clockwise yaw moment is represented in (18).

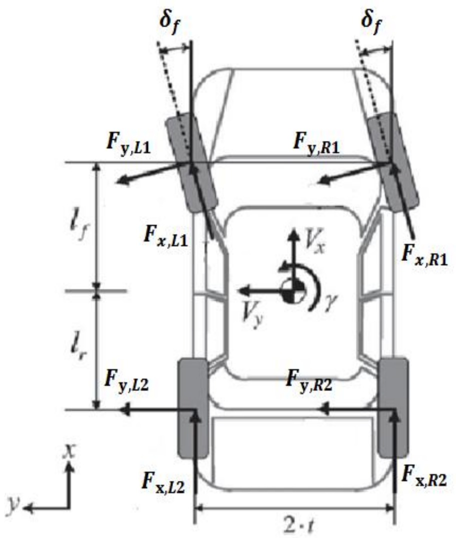

Fig. 4 Planar vehicle model.

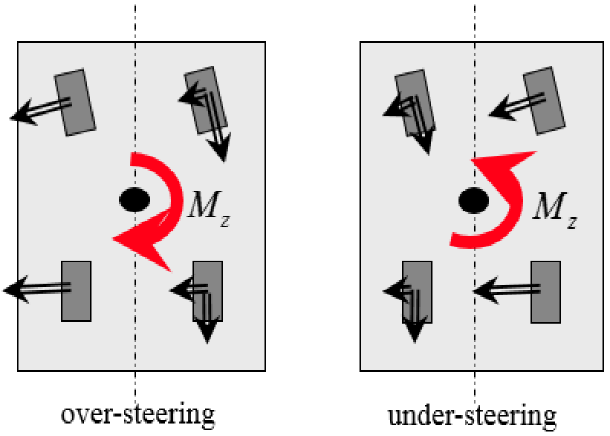

Fig. 5 Correction yaw moment during left turn.

$$M_z + t\cos(\delta_f)\left(\frac{J_\omega\dot{\omega}_{L1}-T_{d,L1}}{R_e}+\mu_r F_{z,L1}-F_{x,R1}\right) \\ +t\left(\frac{J_\omega\dot{\omega}_{L2}}{R_e}+\mu_r F_{z,L2}\right) = \begin{bmatrix}\frac{-t\cos(\delta_f)}{R_e} & \frac{-t}{R_e}\end{bmatrix}\begin{bmatrix}T_{b,L1}\\ T_{b,L2}\end{bmatrix} \quad (18)$$

where

$$\begin{bmatrix}T_{b,L1}\\ T_{b,L2}\end{bmatrix} = \begin{bmatrix}-k_{B1}P_{L1}\\ -k_{B2}P_{L2}\end{bmatrix}$$

k_{B1} and k_{B2} are the front and rear brake gains. P_* denotes brake cylinder pressure of the corresponding wheel. In the same manner, brake distribution for clockwise yaw moment is obtained as follows:

$$M_z - t\cos(\delta_f)\left(\frac{J_\omega\dot{\omega}_{R1}-T_{d,R1}}{R_e}+\mu_r F_{z,R1}-F_{x,L1}\right) \\ -t\left(\frac{J_\omega\dot{\omega}_{R2}}{R_e}+\mu_r F_{z,R2}\right) = \begin{bmatrix}\frac{t\cos(\delta_f)}{R_e} & \frac{t}{R_e}\end{bmatrix}\begin{bmatrix}T_{b,R1}\\ T_{b,R2}\end{bmatrix} \quad (19)$$

where

$$\begin{bmatrix}T_{b,R1}\\ T_{b,R2}\end{bmatrix} = \begin{bmatrix}-k_{B1}P_{R1}\\ -k_{B2}P_{R2}\end{bmatrix}$$

On the contrary, during right turn, the applied brake pressures for preventing over-steer and under-steer shown in Fig. 5 are reversed.

3.2 Control allocation

To determine the brake cylinder pressures in (18) and (19), WLS control allocation method is applied in this section (see Fig. 6).

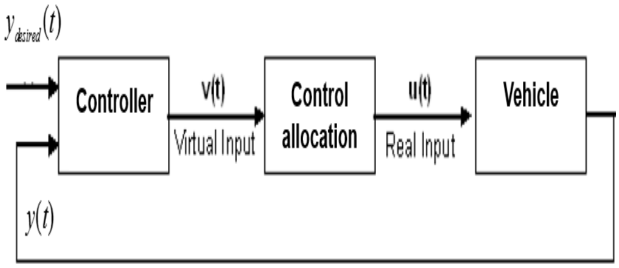

Fig. 6 Diagram of control allocation.

There are some benefits of that: (1) physical limits of the brake pressures are automatically taken into account; (2) in the event that the system failure happens, vehicle stability can be maintained; (3) Optimized brake pressure can be achieved [8]. Consider the cost function with weighting factor γ.

$$J = \|W_u(u-u_d)\|^2 + \gamma\|W_v(Bu-v)\|^2 \qquad (20)$$

where

$$u_d = [0 \quad 0]^T$$

$r - r_d < -\varepsilon$: for counter clockwise moment

$$u = [P_{L1} \quad P_{L2}]^T$$

$$B = \begin{bmatrix} \dfrac{tk_{B1}\cos(\delta_f)}{R_e} & \dfrac{tk_{B2}}{R_e} \end{bmatrix}$$

$$v = M_z + t\cos(\delta_f)\left(\frac{J_\omega \dot{\omega}_{L1} - T_{d,L1}}{R_e} + \mu_r F_{z,L1} - F_{x,R1}\right)$$

$$+ t\left(\frac{J_\omega \dot{\omega}_{L2}}{R_e} + \mu_r F_{z,L2}\right)$$

$r - r_d > \varepsilon$: for clockwise moment

$$u = [P_{R1} \quad P_{R2}]^T$$

$$B = \begin{bmatrix} \dfrac{-tk_{B1}\cos(\delta_f)}{R_e} & \dfrac{-tk_{B2}}{R_e} \end{bmatrix}$$

$$v = M_z - t\cos(\delta_f)\left(\frac{J_\omega \dot{\omega}_{R1} - T_{d,R1}}{R_e} + \mu_r F_{z,R1} - F_{x,L1}\right)$$

$$- t\left(\frac{J_\omega \dot{\omega}_{R2}}{R_e} + \mu_r F_{z,R2}\right)$$

W_u and W_v are weighting matrices. The control input, i.e., brake pressure, is optimized by minimizing the cost function while satisfying the constraints of input.

$$u = \arg\min_{\underline{u} \le u \le \bar{u}} \|W_u(u-u_d)\|^2 + \gamma\|W_v(Bu-v)\|^2 \qquad (21)$$

Understeering: $\underline{u} = [0 \quad 0]^T$

$\bar{u} = [0.3\,MPa \quad 5\,MPa]^T$

Oversteering : $\underline{u} = [0 \quad 0]^T$

$\bar{u} = [3\,MPa \quad 5\,MPa]^T$

Generally, the large front brake forces easily cause the weight shifting. To avoid the unstable vehicle motion from this unexpected weight shifting, the upper bound $\bar{u}$ of the front brake pressure is set to be smaller than rear brake pressure. Usually, since over steering is considered dangerous situation, ESC systems mainly focus on quickly turning the vehicle heading angle for the correct direction of vehicle. On the contrary, understeering is not considered as quite dangerous situation, and therefore, ESC systems are allowed to generate relatively loose brake pressure. The upper bound of front brake pressure are changed to be relatively small value, 0.3 MPa in understeering behavior. This change can lead to the minimum disturbance of longitudinal vehicle motion while ESC systems are implemented.

4. SIMULATION RESULTS

By using Carsim software, the proposed allocation algorithm is evaluated. The vehicle model of simulation is D-class sedan whose parameters are represented in Table 1. The sampling time of the controller is 1 ms. In the simulation environments on high friction coefficient (mu=0.85) surfaces, driving scenario is double lane change known as a harsh scenario for the performance evaluation at the limit of handling [1]. The driving maneuvers are represented in Fig 7. Fig. 8 shows the simulation results on high mu surfaces for 10 seconds simulation time. It is confirmed that the controlled yaw rate with ESC system tracks the desired value well. The yaw rate with ESC system has much smaller errors than that without ESC. Due to the implementation of WLS control allocation, the actual correction yaw moment M_z generated by the brake pressures are very close to the virtual M_z required from the upper controller.

Table 1 Vehicle parameters.

Parameter	Value	Symbol
Mass of vehicle	1370kg	m
CG-front axle distance	1.11m	l_f
CG-rear axle distance	1.666m	l_r
Cornering stiffness of front axle	$1.73\times10^5\,N/rad$	C_f
Cornering stiffness of rear axle	$1.3\times10^5\,N/rad$	C_r
Yaw moment of inertia	$4192\,kg\cdot m^2$	I_z
Wheel inertia	$0.9\,kg\cdot m^2$	J_w
Width of vehicle	1.795m	t
Effective rolling radius	0.33m	R_e
Rolling resistance	0.004	μ_r
Front brake gain	$300m^3$	k_{B1}
Rear brake gain	$150m^3$	k_{B2}

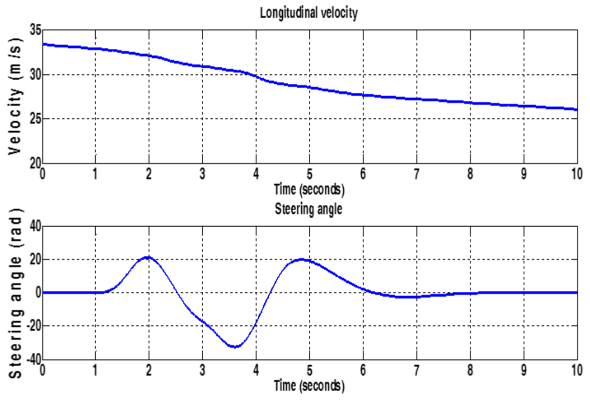

Fig. 7 Driving maneuvers.on high mu surface.

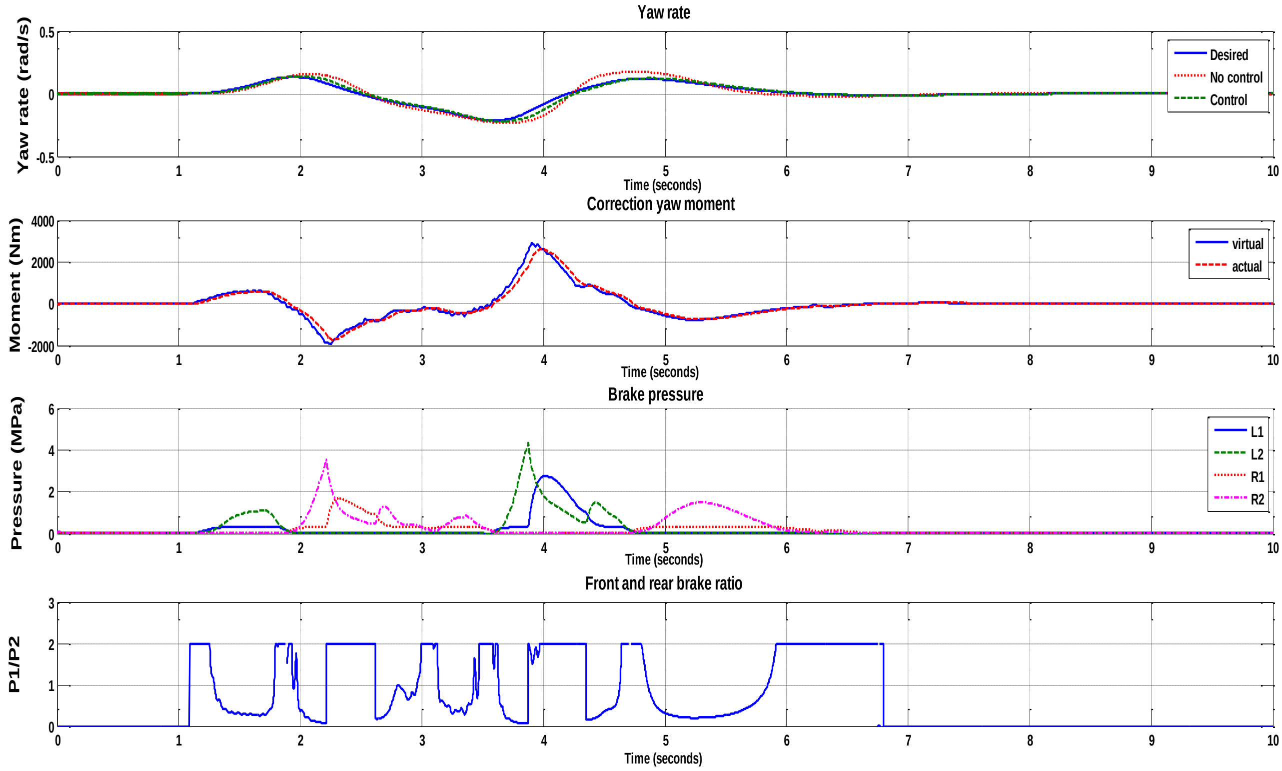

Fig. 8 Simulation results on high mu surface.

Since the actual M_z leads to the high tracking performances, the lateral stability of the vehicle can be maintained. Fig. 8 shows brake pressures of each individual wheel as well as front and rear brake ratio P_1 / P_2. This P_1 / P_2 includes P_{L1} / P_{L2} and P_{R1} / P_{R2}. It is confirmed that the optimized front and rear brake ratio is almost 2 for preventing the oversteering behavior. If this ratio is set to be an arbitrary constant value without the WLS control allocation method, the optimization of brake pressures is difficult to be achieved. Inadequate brake distribution may bring about following issues: 1) ESC systems may generate insufficient brake pressures, and therefore, the vehicle cannot deviate the oversteering behavior; 2) During the understeering behavior, ESC systems may generate excessive brake pressures causing the decreased tire-road adhesion force, and then induce some unstable vehicle motions.

5. CONCLUSIONS

This paper proposes a novel method of optimal distribution of the brake pressures for ESC systems. Also, it is confirmed that WLS control allocation method minimizing the user-defined cost function is a suitable algorithm for development of the proposed ESC systems. With simulations based on harsh scenarios, the effectiveness of algorithm is tested and analysed in detail. As a result, high tracking performance with respect to the yaw rate and optimized distribution of brake pressures are exhibited. In addition, to take vehicle stability into account, the brake actuators have varying constraints depending on the steering cases, oversteering and understeering. In conclusion, the benefits of the proposed algorithm is verified, and also, it is sufficiently worth using for ESC systems of the commercial vehicle. However, to guarantee the real timeness of the control allocation method, a high level ECU is necessary to process a lot of computations. Also, in the future works, the time-delay issues in both the sensing process and the hydraulic brake actuator have to be considered and compensated.

ACKNOWLEDGEMENT

This work was supported by the National Research Foundation of Korea (NRF) grant funded by the Korea government (MSIP) (No.2010-0028680). This research was supported by the MSIP (Ministry of Science, ICT and Future Planning), Korea, under the C-ITRC (Convergence Information Technology Research Center) (ITTP-2016-H8601-16-1005) supervised by the ITTP(Institute for Information & communications Technology Promotion), and the BK21 plus program.

REFERENCES

[1] M. Choi and S.B. Choi, “Model predictive control for vehicle yaw stability with practical concerns,” *IEEE Transactions on Vehicular Technology*, Vol. 63, No. 8, pp. 3539-3548, 2014.

[2] P. Falcone, H.E. Tseng, F. Borrelli, and D. Hrovat, “MPC-based yaw and lateral stabilisation via active front steering and braking,” *Vehicle System*

Dynamics, Vol. 46, pp. 611-628, 2008.

[3] S. Ferguson, “The effectiveness of electronic stability control in reducing real-world crashes: a literature review,” *Traffic Injury Prevention*, Vol. 8, No. 4, pp. 329-338, 2007.

[4] L. Laine and J. Andreasson, “Control allocation based electronic stability control system for a conventional road vehicle,” *Proc. of the 2007 IEEE Intelligent Transportation Systems Conference*, pp. 514-521, 2007.

[5] J. Tjonnas and T. Johansen, “Stabilization of automotive vehicles using active steering and adaptive brake control allocation,” *IEEE Transactions on Vehicular Technology*, Vol. 18, No. 3, pp. 545-558, 2010.

[6] H. Zhou and Z. Liu, “Vehicle yaw stability-control system design based on sliding mode and backstepping control approach,” *IEEE Transactions on Vehicular Technology,* Vol. 59, No. 7, pp. 3674-3678, 2010.

[7] J. Oh and S. B. Choi, “Vehicle velocity observer design using 6-D IMU and multiple-observer approach,” *IEEE Transactions on Intelligent Transportation Systems*, Vol. 13, No. 4, 2012.

[8] O. Harkegard. “Efficient active set algorithms for solving constrained least squares problems in aircraft control allocation,” *Proc. of the 41st IEEE Conference on Decision and Control*, pp. 1295-1300, 2002.

[9] R. Rajamani, *Vehicle Dynamics and Control*. Springer Science & Business Media, 2011.

[10] P.A. Ioannou and J. Sun, *Robust Adaptive Control*. Englewood Cliffs, NJ: Prentice-Hall, 2964.

[11] H. Pacejka, *Tire and vehicle dynamics*. Elsevier, 2005.